Turkish Journal of Engineering

Turkish Journal of Engineering (TUJE)
Vol. 4, Issue 4, pp. 183-196, October 2020
ISSN 2587-1366, Turkey
DOI: 10.31127/tuje.639378
Research Article

AN EXTENDED ANALYSIS OF THE MODELS TO ESTIMATE PHOTOVOLTAIC MODULE TEMPERATURE

Talat Ozden *[1,2], Doga Tolgay [3,4], M. Samet Yakut [4] and Bulent G. Akinoglu [3,4,5]

[1] Gumushane University, Department of Energy Systems Engineering, Gumushane, Turkey
[2] METU, The Center for Solar Energy Research and Applications (GUNAM), Ankara, Turkey
ORCID ID 0000 – 0002 – 0781 – 2904
tozden@gumushane.edu.tr

[3] METU, Department of Physics, Ankara, Turkey
[4] METU, Department of Electrical and Electronics Engineering, Ankara, Turkey
ORCID ID 0000 – 0002 – 3155 - 946X
doga.tolgay@metu.edu.tr

[4] METU, Department of Electrical and Electronics Engineering, Ankara, Turkey
ORCID ID 0000 – 0002 – 3236 – 5843
samet.yakut@metu.edu.tr

[3] METU, Department of Physics, Ankara, Turkey
[4] METU, Department of Electrical and Electronics Engineering, Ankara, Turkey
[5] METU, Earth System Science Program, Ankara, Turkey
ORCID ID 0000 – 0003 – 1987 – 6937
bulo@metu.edu.tr

* Corresponding Author
Received: 29/10/2019 Accepted: 07/01/2020

ABSTRACT
To estimate the performance of the photovoltaic power systems is the key issue in their techno-economic feasibility analysis. Performances, on the other hand, strongly depends on the module temperatures of the photovoltaic systems. In this study, we evaluated the performance of ten different module temperature estimation models using the measured outdoor data of five different modules. The modules are installed at the rooftop of a building located at Central Anatolia where the climate is cold and semi-arid. The results showed that the models having smaller number of parameters perform better than the others. We concluded that such analysis should be carried out at different ambient conditions so that the best performing models for the site can be obtained. Another outcome of the study is that the seasonal evaluation of the performance of the models should be carried out.

Keywords: *Photovoltaic Module, Module Temperature, Module Temperature Variation, Module Temperature Estimation*

1. INTRODUCTION

The interest in renewable energy resources is growing due to the environmental damages of fossil fuels. So nowadays, many power plants that use renewable energy resources such as hydro, wind and solar, etc. have been installed worldwide in the last decades. Especially, solar power plants installments are rapidly growing all over the world. Reports published by International Renewable Energy Agency (IRENA, 2019) and International Energy Agency (IEA, 2019) in 2019 show that total installed photovoltaic (PV) capacity reaches nearly 500 GWp. Also, the same report (IRENA, 2019) shows that the PV capacity in Turkey reaches 5 GWp during just the last three years. According to another report, including some scenarios (SolarPowerEurope 2018), this installation trend will continue at the same rate till 2022. For example, installation PV capacity in the world will be 1.2 TWp as regards to high scenarios or will be 813 GWp as regards to low scenarios.

While the installation of solar power plants increasing with a large rate, the R&D on the subject matter interestingly also heavily keeps going. In this respect, the performance of the solar modules particularly depends on the module temperature and thus, it becomes important to estimate the module temperature for short- and long-term feasibility analyzes. There exist in the literature many correlations connecting the module temperature to climatic parameters and datasheet specifications of the modules.

It is obvious that a considerable amount of solar energy absorbed by solar panels is converted into heat within the cell. Then, the temperature of the PV modules increases due to heat. Researchers conducted several studies to see how the temperature affects the efficiency of the modules. According to Dubey *et al*, efficiency is linearly decreasing with operating temperature (cell or module temperature) (Dubey, Sarvaiya, and Seshadri, 2013). A research conducted on this issue by Rahman *et al*. illustrated that each 1°C increase in cell temperature causes a 0.06% decrease in electrical efficiency of the PV module under solar irradiance of 1000 W/m^2 (Rahman, Hasanuzzaman, and Rahim, 2015). Another research which was conducted by Amr *et al*. shows that the temperature of the modules can be decreased using heat sink fins thermally attached to the back surface of the modules (Amr *et al*., 2019). They calculated the module temperature using a thermal modeling approach and conducted experiments to compare their results.

The efficiencies of solar cells are measured at standard test conditions where cell temperature is 25 °C and irradiance 1000 W/m^2. However, solar cells are rarely meet this standart efficiency value at outdoor conditions, because on a clear summer day the temperature of PV panels can reach up to 60 °C (Ozden, Tolgay, and Akinoglu, 2018). Therefore, to forecast the yield before solar power plant installation, it is also necessary to estimate the module temperature. There exist many temperature estimation correlations from various authors in the literature (Duffie and Beckman, 2013; Eckstein, 1990; Faiman, 2008; King, Boyson, and Kratochvil, 2004; Koehl *et al*., 2011; Kurtz *et al*., 2009; Mattei *et al*., 2006; Roberts, Zevallos, and Cassula, 2017; Santhakumari and Sagar, 2019).

Skoplaki *et al*. indicated that free convection loss is insignificant when compared to wind convection loss for wind speed 1-15 m/s. They obtained that the average deviation between measured and estimated Tc values is less than 3 °C in the range 1–15 m/s (Skoplaki, Boudouvis, and Palyvos, 2008).

Mattei *et al*. used two different temperature equations and found that after 10 m/s wind speed effect becomes less important in terms of yield per meter square (Mattei *et al*., 2006). Eckstein estimated the module temperature in his thesis by using a loss temperature coefficient (Eckstein, 1990). M. Akhsassi *et al*. developed two temperature equations, one can be used with wind speed data and the other can be used without wind data. They have used 32 monocrystalline silicon panels and calculated overall lost coefficients for the panels. Moreover, they have analyzed different types of thermal models. In their analysis, they have found that Sandia and Faiman temperature model overestimates the PV module temperature when irradiance is high and underestimates the module temperature when irradiance is low whereas Lasnier thermal model underestimates module temperature when irradiance is high and overestimates when irradiance is low (Akhsassi *et al*., 2018). Gökmen *et al*. investigated two different thermal models; one of them considers the cooling effect of wind whereas the other one does not consider. The authors estimated yearly energy values using predicted module temperature from these models and measured module temperature from a PV system, including Poly-Si modules at the windy location Aalborg, Denmark. The study presented that formula (does not consider the wind speed data) underestimates the yearly energy by 3.5% since it overestimates the module temperature (Gökmen *et al*., 2016).

Dierauf *et al*. have developed a formula differing from traditional ones. Their new thermal model estimates the temperature by considering the effects of the ambient temperature and wind (Dierauf *et al*. 2013). Another temperature formula developed by Ding *et al*. calculates the cell temperature with the help of the back surface temperature of the modules (Ding *et al*. 2014). Lo Brano *et al*. acquired a formula that is sensitive to irradiance and temperature changes by calculating K factor which is thermal correction factor (Lo Brano and Ciulla 2013). Skoplaki and Palyvos analyzed 22 different temperature models and came up with the fact that use of these models should be handled with care as they are developed for specific mounting geometry or building integration level (Skoplaki and Palyvos 2009). Schwingshackl *et al*. worked on four different temperature models of standard approach namely Skoplaki's, Koehl's, Mattei's and Kurt's models. They found out that models which include wind cooling effects can be used for better estimations (Schwingshackl *et al*. 2013).

This study gives the analysis of measured data of module temperatures for five modules tested in outdoor conditions of a cold semi-arid climate of Ankara. The modules are tested for three years. Ten models from the literature are chosen for a comparative study to reach the best-performing ones to be used in techno-economic analysis.

The next section gives the materials and methods used in work together with a description of the site, climate, data, and the models. Section three gives the results of the analysis, and the statistical errors are tabulated and discussed. The last section is concluding remarks with some future prospects.

2. MATERIALS AND METHOD

2.1. Description of Sites and Modules

Measurements are taken on the rooftop of METU, Department of Physics building in Ankara, Turkey which was located in the Central Anatolia. According to Köppen - Geiger Climate Classification, Ankara has a cold semi-arid climate (Peel, Finlayson, and McMahon, 2007; Rubel *et al*., 2017).

The technical details of test sites are presented in Table 1. They are in operation for three years between April 2016 to April 2019. The average ambient temperature in this time interval is 13.8 °C. The highest temperature is 38.5 °C in July 2017 and the lowest temperature is −8.9 °C in February 2017 during the test period. And also, annual average relative humidity (RH) and wind speed is about 60 % and about 1 m/s, respectively.

Table 1. Test site details

Parameter	GUNAM-Ankara, Turkey
Latitude (°N)	39.9
Longitude (°E)	32.8
Elevation (m)	929
Tilt & Azimuth angle (°)	32 & 0

Five different types of PV modules are investigated in this study. Modules are mounted on an aluminum construction and they are not close to each other. Two of the tested PV modules which are microcrystalline based amorphous silicon (μc-Si/a-Si) and Cupper Indium Selenide (CIS) are thin film. The other three PV modules have crystalline silicon structures which are Monocrystalline Silicon (Mono-Si), Polycrystalline Silicon (Poly-Si) and Heterojunction with Intrinsic Thin layer (HIT). They are cleaned weekly.

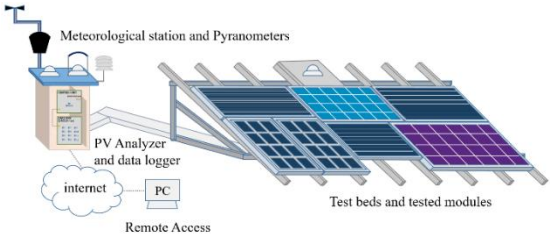

(a)

(b)

Fig. 1. Configuration of METU-GUNAM Outdoor Test Facility (a) and tested modules - 1: CIS, 2: Poly-Si, 3: Mono-Si, 4: μc-Si / a-Si, 5: HIT (b)

The elements of our testing system can be seen in Fig. 1 and the specifications of five tested modules used in the present study are tabulated in Table 2.

Table 2. Tested PV Modules Specifications

Module Types	P_{MAX} [W]	V_{OC} [V]	I_{SC} [A]	V_{MPP} [V]	I_{MPP} [A]	η [%]	β_{STC} [%/°C]	$T_{m,NOCT}$ [°C]	Area [m2]
CIS	130.0	59.50	3.28	44.90	2.90	12.3	-0.39	40	1.05
Mono-Si	160.0	43.70	5.06	35.30	4.58	12.5	--**	--**	1.28
Poly-Si	130.0	21.70	8.18	17.80	7.30	12.7	-0.45*	46	1.02
μc-Si / a-Si	128.0	59.80	3.45	45.40	2.82	9.1	-0.24	44	1.40
HIT	230.0	42.30	7.22	34.30	6.71	16.5	-0.30	45	1.39

* The parameter unit is %/K. ** There is no datasheet for this module. Therefore, some results are missing.

2.2. Receiving Data from the Test Setup

All of the modules are connected to a PV analyzer which measures the electrical performance, solar radiation, and module and ambient temperatures. The average measurement results of these parameters are taken in every 10 minutes and are saved inside a daily file to the internal memory of the analyzer. Solar irradiation is measured by using a Kipp&Zonnen high precision secondary standard pyranometer, and temperatures data are measured by using T type thermocouples. The thermocouples which are used for measurement of cell temperatures are firmly adhered to at the back of each module. These temperature sensors are attached to the middle of the modules (Fig. 2). However, as the junction box of the μc-Si / a-Si module is located at the center of the module backside, the thermocouple of this module is adhered to near its junction box (Ozden, Tolgay, and Akinoglu, 2018)

Climatic parameters are measured with a meteorological station. The station can measure ambient temperature, RH, precipitation, solar irradiance, wind speed, and direction every 10 minutes time interval. The station is fixed to 2 meters above from the floor level of the rooftop.

Fig. 2. One of the temperature sensors adhered to the backside of a module

The module temperatures reach about 70 °C under around 1000 W/m^2 of irradiance and at elevated ambient temperature except for the μc-Si / a-Si thin-film module. The corresponding values for the μc-Si / a-Si stay somewhat at 60 °C at the same conditions.

2.3. Approaches Used in PV Temperature Estimation

In the study, ten correlations presented in the literature are used to estimate the module/cell temperature from ambient temperatures and some other parameters (see Table 3). These equations are mainly tested and suggested to estimate the module/cell temperature in literature. Besides, some software packages for performance analysis of PV systems also use some of these equations (Homer Pro 3.13 help documentation, 2019; PVsyst 6 help documentation, 2019). To estimate the module temperature, Homer Pro uses Eq. 5 and PVsyst uses Eq. 1 in Table 3.

Presented equations in Table 3 contain many parameters. Some are the same while some differ. The explanation of these parameters is given in the Nomenclature section. However, values of some of these parameters (such as parameters with STC and NOCT indexing) are obtained from the datasheet of modules supplied by the manufacturer. The other parameter values are taken from the references explained in the followings.

Table 3. Several correlations to estimate the cell or module temperature.

Eq. #	Correlation	Ref
1	$T_m = G_t \times e^{(a+bV_w)} + T_a$	(King *et al*., 2004)
2	$T_c = T_a + \frac{G_t(T_{m,NOCT} - T_{a,NOCT})}{G_{NOCT}}$	(Ross and Smokler, 1986)
3	$T_m = T_a + \frac{G_T}{U_0 + U_1 V_w}$	(Faiman, 2008)
4	$T_c = \frac{U_{PV}T_a + G_t(\alpha\tau - \eta_{STC} - \beta_{STC}\eta_{STC}T_{STC})}{U_{PV} - \beta_{STC}\eta_{STC}G_t}$	(Sandnes and Rekstad, 2002)
5	$T_c = T_a + \frac{G_t\alpha\tau}{U_L}\left(1 - \frac{\eta_{STC}}{\alpha\tau}\right)$	(Eckstein, 1990)
6	$T_c = T_a + \frac{G_t(T_{m,NOCT} - T_{a,NOCT})}{G_{NOCT}}\left[1 - \frac{\eta_{STC}}{\alpha\tau}\right]\frac{h_{w,NOCT}}{h_w}$	(Duffie and Beckman, 2013)
7	$T_c = T_a + \frac{G_t(T_{m,NOCT} - T_{a,NOCT})}{G_{NOCT}}\left[1 - \frac{\eta_{STC}(1 - \beta_{STC}T_{m,STC})}{\alpha\tau}\right]\frac{h_{w,NOCT}}{h_w}$	(Akhsassi *et al*., 2018)
8	$T_c = T_a + \omega \times \left(\frac{0.32}{h_w}\right) \times G_t$	(Skoplaki *et al*., 2008)
9	$T_m = \frac{T_a + \frac{G_t}{G_{NOCT}} \times (T_{m,NOCT} - T_{a,NOCT}) \times \frac{h_{w,NOCT}}{h_w} \times \left(1 - \frac{\eta_{STC}}{\alpha\tau} \times (1 - \beta_{STC} \times T_{STC})\right)}{1 - \left(\frac{\beta_{STC}\eta_{STC}}{\alpha\tau}\right) \times \left(\frac{G_t}{G_{NOCT}}\right) \times (T_{m,NOCT} - T_{a,NOCT}) \times \frac{h_{w,NOCT}}{h_w}}$	(Skoplaki *et al*., 2008)
10	$T_m = \omega_1 \times T_a + \omega_2 \times G_t + \omega_3 \times V_w + c$	(Tamizhmani *et al*., 2003)

In Eq. (1), a and b constants are taken from reference (King, Boyson, and Kratochvil, 2004). They are taken as −3.47 and −0.0594 for CIS module due to its module structure (glass/cell/glass and open rack) whereas for the other modules they are taken as −3.56 and −0.075 because of their module structure and fixing position (glass/cell/polymer sheet and open rack), respectively. In the same equation, the wind speed V_w was measured at a standard height of 10 m. However, the wind speed was not measured at a height of 10 m in our test site. Therefore, the wind speed value was converted to the appropriate height using the measurement height by the following power law (Twidell and Weir, 2015):

$$\frac{V_w}{V_{w,ref}} = \left(\frac{z}{z_{ref}}\right)^n \quad (13)$$

where z_{ref} is reference height measured from the ground,

z is 10 m and $V_{w,ref}$ is the measured wind speed at the height of the test site. n is the friction coefficient and the coefficient is a function of the topography at the test site (small town with some trees and shrubs). It is taken as 0.3 from (Bañuelos-Ruedas, Angeles-Camacho, and Rios-Marcuello, 2010). In Eq. (3), U_0 and U_1 constants are taken as 23.09 and 3.11 for the CIS module from (Koehl *et al*., 2011) and taken as 25 and 6.84 for the other modules from (Faiman, 2008), respectively. The Eq. (6, 7, 8 and 9) include the heat convection coefficient equations. The correlations to estimate module/cell temperature in the literature use many parameters of climatic conditions and its nameplate parameters (Cole and Sturrock, 1977; Duffie and Beckman, 2013; Kaplani and Kaplanis, 2014; Loveday and Taki, 1996; Nolay, 1987; Sharples and Charlesworth, 1998). Some of them are frequently chosen for more accurate estimation of module/cell temperature and are tabulated in Table 4. The coefficients of Eq. 12, 20, 16 and 16 in Table 4 are used In Eq. 6, 7, 8 and 9 (like $h_w = 5.7 + 3.8V_w$ and $h_{w,NOCT} = 5.7 + 3.8V_{w,NOCT}$), respectively.

Table 4. Various air forced heat convection coefficient equations ($\boldsymbol{h_w}$ ***and*** $\boldsymbol{h_{w,NOCT}}$)

	Heat convection coefficients	Eq. #	Ref
1	$\boldsymbol{h_w = 5.67 + 3.86V_w}$	12	(Duffie and Beckman 2013)
2	$\boldsymbol{h_w = 5.82 + 4.07V_w}$	13	(Nolay 1987)
3	$\boldsymbol{h_w = 11.4 + 5.7V_w}$ for the windward condition	14	(Cole and Sturrock 1977)
4	$\boldsymbol{h_w = 5.7}$ for the leeward conditions	15	(Cole and Sturrock 1977)
5	$\boldsymbol{h_w = 8.91 + 2.0V_w}$ for the windward condition	16	(Loveday and Taki 1996)
6	$\boldsymbol{h_w = 4.93 + 1.77V_w}$ for the leeward conditions	17	(Loveday and Taki 1996)
7	$\boldsymbol{h_w = 8.3 + 2.2V_w}$ for the windward condition (angle 0°)	18	(Sharples and Charlesworth 1998)
8	$\boldsymbol{h_w = 7.9 + 2.6V_w}$ for the windward condition (angle 45°)	19	(Sharples and Charlesworth 1998)
9	$\boldsymbol{h_w = 6.5 + 3.3V_w}$ for the windward condition (angle 90°)	20	(Sharples and Charlesworth 1998)
10	$\boldsymbol{h_w = 7.9 + 2.2V_w}$ for the windward condition (angle 135°)	21	(Sharples and Charlesworth 1998)
11	$\boldsymbol{h_w = 8.3 + 1.3V_w}$ for the windward condition (angle 180°)	22	(Sharples and Charlesworth 1998)

U_{PV} is the heat exchange coefficient corresponding to the total surface area of the module, i.e. two times the surface area corresponding to h_w since the heat is lost from the two faces of the PV (lateral surfaces are neglected) (Mattei *et al*., 2006), so if Eq. (12) is used,

$$U_{PV} = 11.34 + 7.72V_w. \quad (23)$$

If Eq. (13) is used,

$$U_{PV} = 11.64 + 8.14V_w. \quad (24)$$

If Eq. (14) and (15) is used,

$$U_{PV} = 17.10 + 5.70V_w. \quad (25)$$

The coefficients of Eq. (23), (24) and (25) are used in Eq. (4) one by one. However, as the best results are obtained by using Eq. (25) together with Eq. (4), just these results are presented in Fig. A4 and in Table 5.

In Eq. (5), U_L is calculated for every module by using Eq. (14) from (Eckstein, 1990).

$$U_L = \frac{G_{NOCT} \times \alpha\tau}{T_{m,NOCT} - T_{a,NOCT}} \quad (14)$$

In addition, in Eq. (4, 5, 6, 7 and 9) $\alpha\tau$ constant are used as 0.9 (Eckstein, 1990; Sandnes and Rekstad, 2002). Another parameter ω in Eq. (8) is taken as 1.0 from (Skoplaki, Boudouvis, and Palyvos, 2008). Though, this equation does not estimate the module temperature when the wind speed equal to zero (Skoplaki, Boudouvis, and Palyvos, 2008). The last parameters in Eq. (10) ω_1, ω_2, ω_3, and c are taken from (Schwingshackl *et al*., 2013) which is presented at a table as average values for every module types.

As the next step to determine and to show which equation has higher accuracy is conducted using two procedures. One of them is that the deviation between estimated and measured values are calculated by using Eq. (26), and these temperature differences are presented as a daily base by using graphics.

$$T_{error} = T_{measured} - T_{estimated} \quad (26)$$

The other method is the use of statistical errors between estimated and measured values evaluated by using mean absolute error (MAE) and root mean squared error (RMSE) methodologies (Eq. (27) and (28)):

$$MAE = \frac{1}{N}\sum_{i=1}^{N}\left|T_{error,i}\right| \quad (27)$$

$$RMSE = \sqrt{\frac{1}{N}\sum_{i=1}^{N}\left(T_{error,i}\right)^2} \quad (28)$$

where N is the total number of data and i is a loop indexing number. The obtained results are tabulated in Table 5.

3. RESULTS AND DISCUSSION

To accurately determine the yield of PV systems is important, and this can only be achieved with the correct prediction of the module temperature. The estimation of module temperature could be made by using implicit and explicit correlations. The implicit correlations generally include thermal and physical properties of the PV

cell/module, solar resource, climatic data, and heat convection coefficient because of the wind. The explicit correlation equations for the operating temperature of the PV cell/module are simply associated with the ambient temperature and the solar irradiance. In this study, to evaluate the accuracy of estimations for some of both types of correlation forms from the literature are selected and used. These equations given in Table 3 are particularly preferred from those in which the best results are obtained in the literature. The ten equations to estimate the PV cell/module temperature for the five different module types are compared using the measured data of three years for these module types. The deviations between estimated and measured data are shown in Appendix. Considering all results, the deviation temperatures can be up to +20 and −30 °C. The best results are obtained from Eq. (1) for a-Si / µc-Si, Poly-Si, and HIT modules and Eq. 8 for CIS and Mono-Si modules. These results have the smallest deviations as can be seen in Fig. A1 and A8, and Table 5. On the other hand, the equations giving the highest deviations for the same modules are from Eq. (4) and Eq. (10). These results are also shown in Fig. A4 and A10, and Table 5.

Table 5. Values of the statistical coefficients for various models[1]

# of T_m estimation Eq.		a-Si / µc-Si	CIS	Mono-Si	Poly-Si	HIT
1	MAE	2.7001	2.4712	2.6520	3.0282	2.8054
	RMSE	3.2746	3.1084	3.2597	3.6006	3.3831
2	MAE	3.6931	2.7175	--*	3.9268	3.6153
	RMSE	4.8522	3.4281	--*	4.7377	4.3805
3	MAE	3.9724	3.8277	3.0817	3.7438	3.6682
	RMSE	5.2178	4.9844	3.8253	4.4985	4.4605
4	MAE	4.9210	3.3601	--*	4.3650	3.9545
	RMSE	6.8621	4.4737	--*	5.4310	4.9395
5	MAE	3.1253	3.0747	--*	3.2659	2.9382
	RMSE	3.9926	4.0215	--*	3.9058	3.5223
6	MAE	3.5149	3.2200	--*	3.8415	3.4405
	RMSE	4.8276	4.2467	--*	4.8189	4.3101
7	MAE	3.2977	3.1766	--*	3.3938	3.1979
	RMSE	4.3417	4.1793	--*	4.0938	3.9130
8	MAE	3.5126	2.2913	2.4232	2.9674	2.9275
	RMSE	4.5885	3.0352	3.1016	3.6376	3.5810
9	MAE	3.2429	2.8345	--*	3.4883	2.8625
	RMSE	4.0496	3.6073	--*	4.1526	3.4589
10	MAE	4.8815	4.3371	4.2181	5.8809	--**
	RMSE	5.4806	5.0573	4.9287	6.5913	--**

* There is no datasheet for this module. Therefore, some results are missing.
** There are no coefficients of Eq. (10) for the HIT module. Therefore, the results are missing.
The best-performing results. The lowest-performing results.

The correlation Eq. (10) presented by NREL in 2003 have high estimation deviation especially during night time. This is probably due to the fact that the coefficients of the correlation are site and climate depended.

As mentioned before, the equations giving the best results are Eq. (1) and (8). Both equations are similar in their structure, one of them has a heat convection coefficient whereas the other equation does not have this coefficient, but instead it has wind speed data which is related to the convection coefficient.

The Eq. (2), (6), (7) and (9) all have similar terms containing STC/NOCT values taken from the datasheets. However, they contain differing additional terms. They all have higher deviations than Eq. (1) and (8) which may be an indication on the weak correlation of the outdoor performances of the modules on their standard parameters given in the datasheet.

The performance of the remaining equations (3) and (4) do not perform well as the others. Finally, Eq. (5) interestingly gives the best results after Eq. (1) for the a-Si / µc-Si and the HIT modules and better than Eq. (8) for the other modules, but the differences are not quite significant. Thus, Eq. (5) could be accepted to be the best to use in the prediction of the yield of a PV power plant.

Fig. 3a, b, and c give three typical days of clear, partially cloudy and overcast sky for comparison of the

best- (either of Eq. (1) or (8)) and lowest-performing (either of Eq. (4) or (10)) estimation models at different irradiation conditions. For the clear day in July for both of the models the estimation results highly fluctuate for the irradiance values between 400 and 1100 W/m^2. The fluctuations for the best-performing model are lower for the HIT and the a-Si / µc-Si and for the lowest-performing model for the other modules. Possible reasons may be the sensitivity of the structure of the models to the variations of the parameters of different type modules. The lowest-performing model overestimates while the best-performing model underestimates in general and this information may be used for further modification of the models.

The best- and lowest-performing models both seem better performing for the partially cloudy day of May (Fig. 3b) except the a-Si / µc-Si module. Hence, in the irradiance ranges of 400-600 W/m^2 the models perform better, so in modest (lower solar irradiance) climatic conditions the estimations are better than in clear sky conditions, and this will further be demonstrated in the following for the overcast sky day.

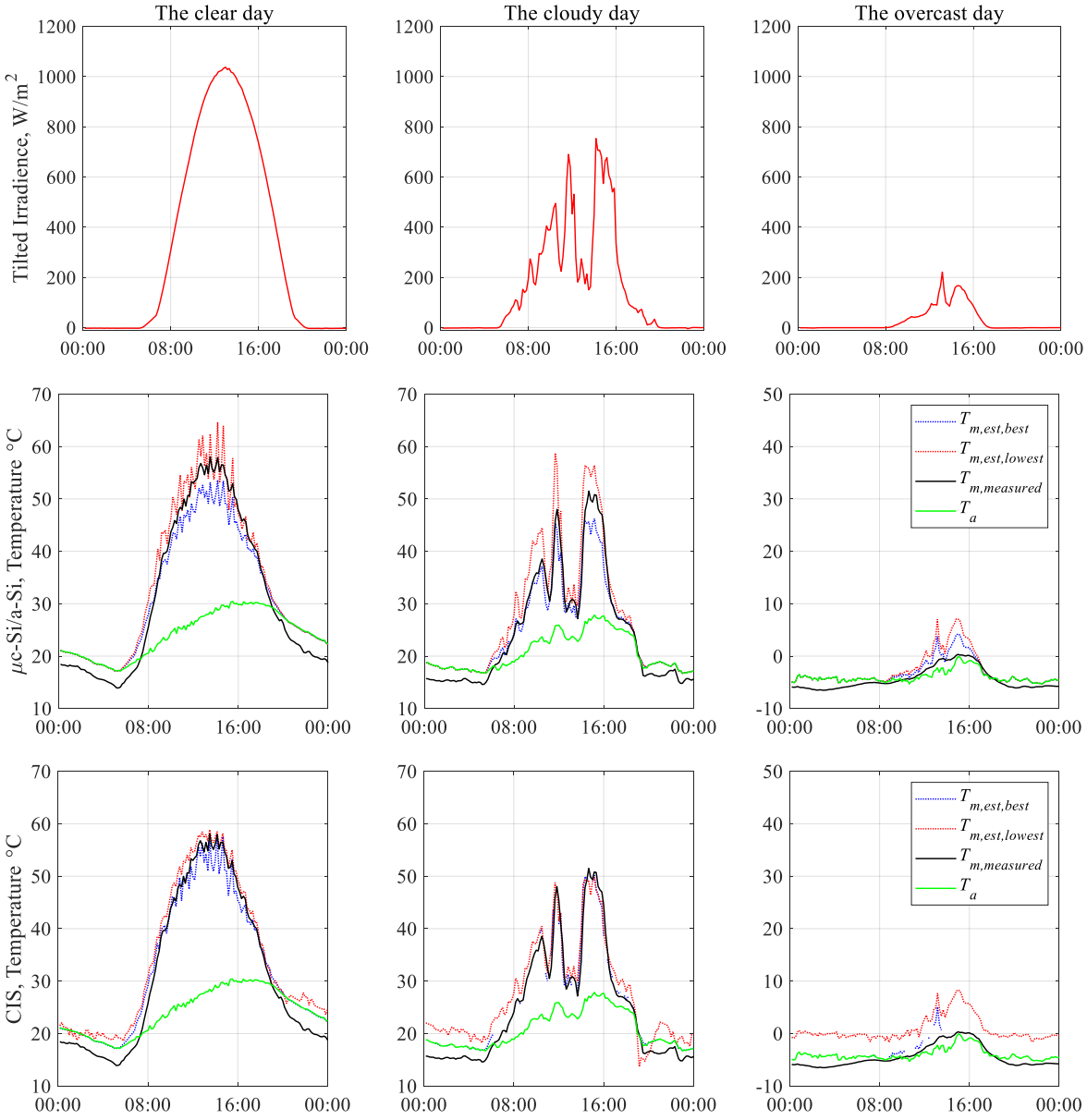

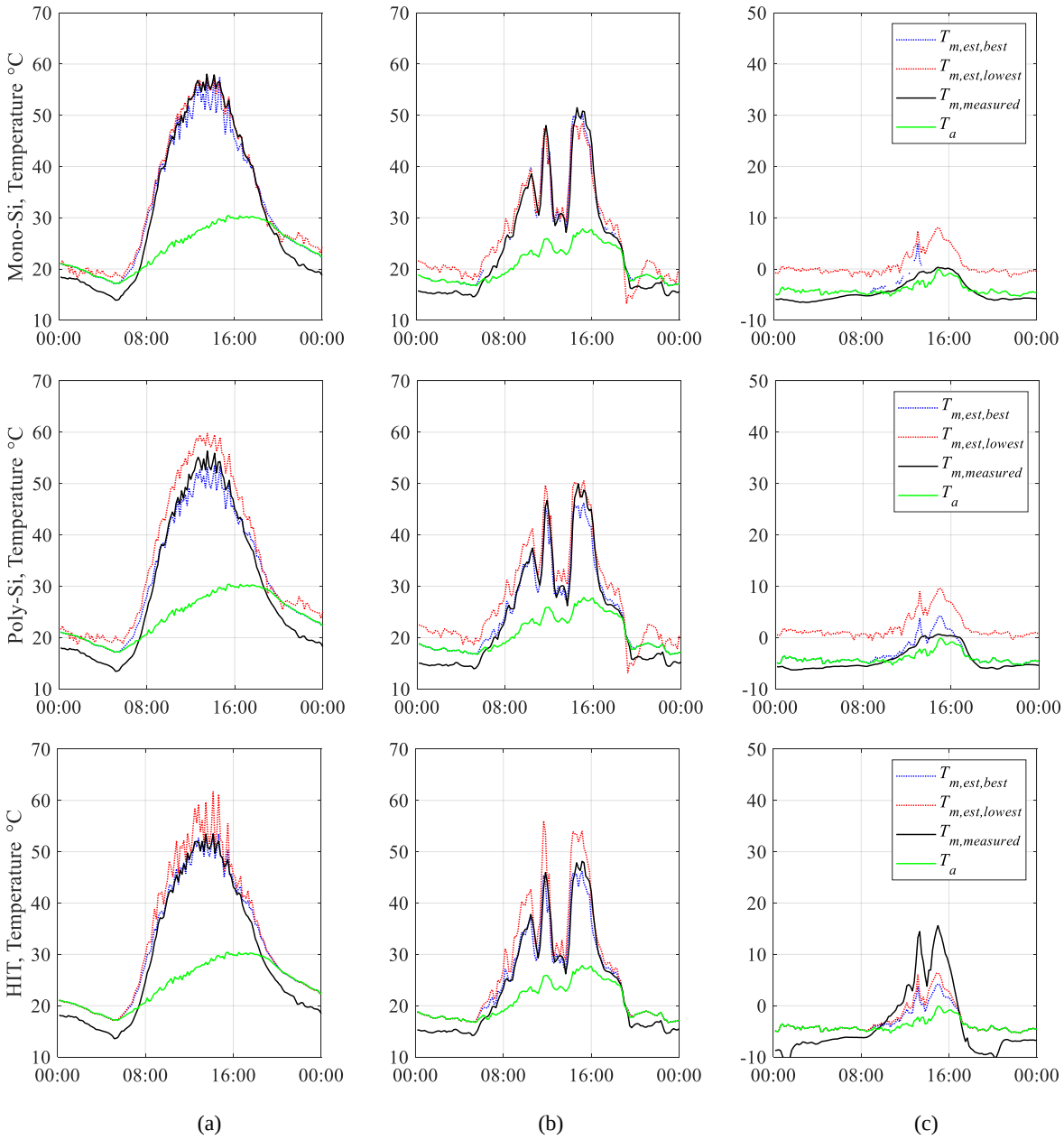

Fig. 3. Comparison measured module temperatures with estimated module temperatures corresponding to best- and lowest-performing results of all module types from Table 5.

The overcast sky of the day in January (Fig. 3c) the irradiance values do not exceed 200 W/m^2, and the ambient temperature is always below 0 °C. The module temperatures are also very low which can be attributed to the very low or no module yields. That is, the module temperature simply follows the ambient temperature closely and the difference is due to thermal response of the module structures under equilibrium conditions. The best-performing model for the CIS and the Mono-Si (Eq. (8)) does not make predictions for hours with zero wind speed, so the predictions are missing for some of the hours of this specific day.

4. CONCLUSIONS

Prediction of the module temperature is very important in the techno-economic analysis of the PV power plants to estimate the yields. There are many models appeared in the literature for the module temperature predictions. In the present study three years measured module temperatures of the five modules tested in outdoor conditions are analyzed. We have chosen ten models from the literature which are commonly used and constructed for all module types and compared their performances.

The models having a smaller number of parameters (Eq. (1) and (8)) perform better than the others for different modules, and this may be attributed to the various climatic conditions that the data were collected to construct the models. That is, larger the number of parameters/coefficients larger the variations of these parameters at different conditions. Eq. (5), which also has

smaller number of parameters/coefficients, seems the best in general than the others, for all the module types. On the other hand, we can state that the prediction performance of the other models also seems acceptable.

This work is performed using the outdoor performance data of the modules under cold and semi-arid climate of Central Anatolia. Such analyses should be carried out for different climates to decide on the best performing model for different climatic conditions. Another further research topic is to carry out the analysis to consider the seasonal variations in the performances of the models to reach better yield estimation calculations.

ACKNOWLEDGMENTS

The authors acknowledge the support given by the Ministry of Development for the construction of the outdoor testing facility.

NOMENCLATURE

a	Empirically-determined coefficient establishing the upper limit for module temperature at low wind speeds and high solar irradiance ($dimensionless$)	τ	Transmittance coefficient ($dimensionless$)
α	Absorptance coefficient ($dimensionless$)	T_a	Ambient temperature ($°C$)
b	Empirically-determined coefficient establishing the rate at which module temperature drops as wind speed increases (s/m)	$T_{a,NOCT}$	Ambient temperature at NOCT ($°C$)
β_{STC}	Temperature coefficient of P_{mpp} ($1/°C$)	T_c	Cell temperature ($°C$)
η_{STC}	Efficiency at STC ($dimensionless$)	T_m	Module temperature ($°C$)
G_{NOCT}	Irradiance at NOCT (W/m^2)	$T_{m,NOCT}$	Module temperature at NOCT ($°C$)
G_t	Solar radiation flux on module plane (W/m^2)	$T_{m,STC}$	Module temperature at STC ($°C$)
h_w	Air forced heat convection coefficient, (KWm^{-2})	U_0, U_1	A coefficient describing the effect of the radiation on the module temperature ($W/m^2°C$), A coefficient describing the cooling by the wind ($Ws/m^3°C$)
$h_{w,NOCT}$	Air forced heat convection coefficient at NOCT, (KWm^{-2})	U_L	Overall thermal loss coefficient ($Wm^{-2}/°C$)
ω	Mounting coefficient ($dimensionless$)	U_{PV}	Heat exchange coefficient for total PV surface area (K/Wm^{-2})
ω_1, ω_2, ω_3, c	Correlation constants, ($dimensionless$, $°C/Wm^{-2}$, $°C/ms^{-1}$, $°C$)	V_W	Wind speed (m/s)

APPENDIX

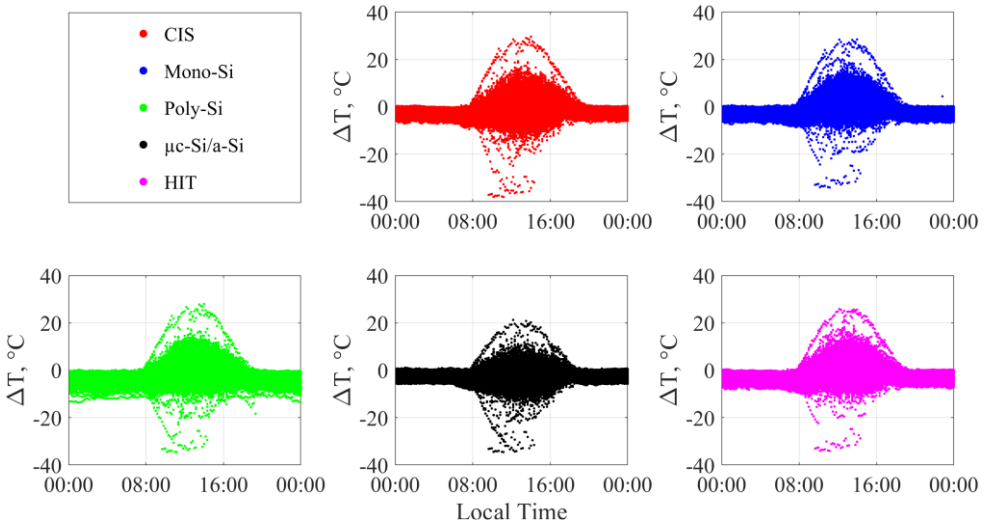

Fig. A1. Difference of module temperatures measured and estimated with Eq. (1).

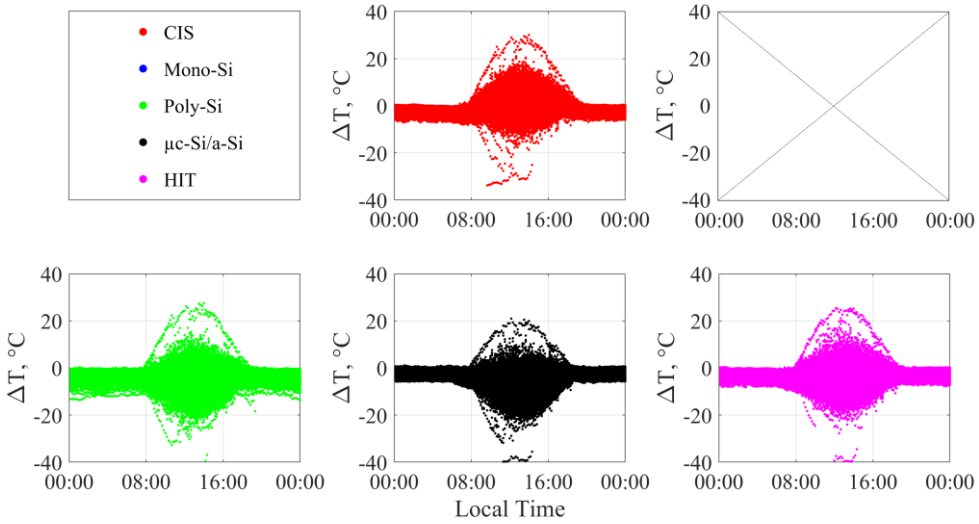

Fig. A2. Difference of module temperatures measured and estimated with Eq. (2).

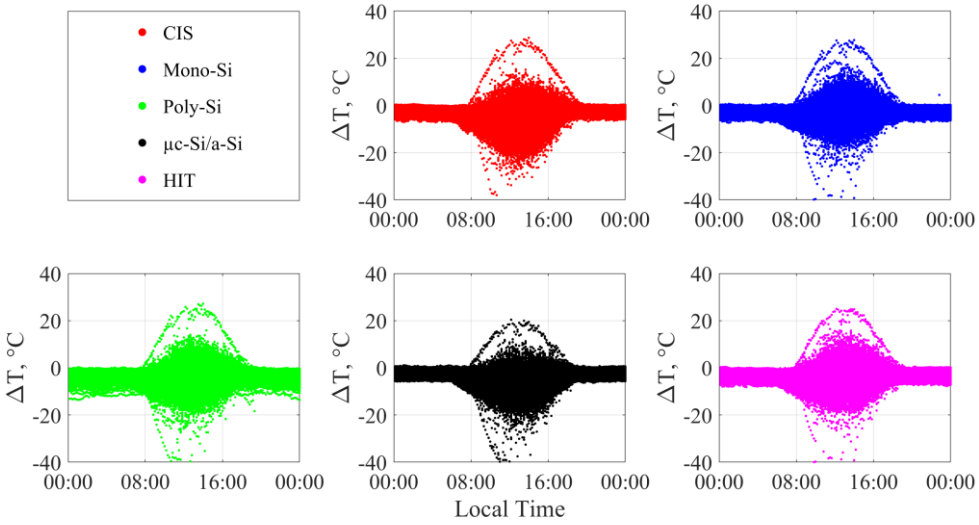

Fig. A3. Difference of module temperatures measured and estimated with Eq. (3).

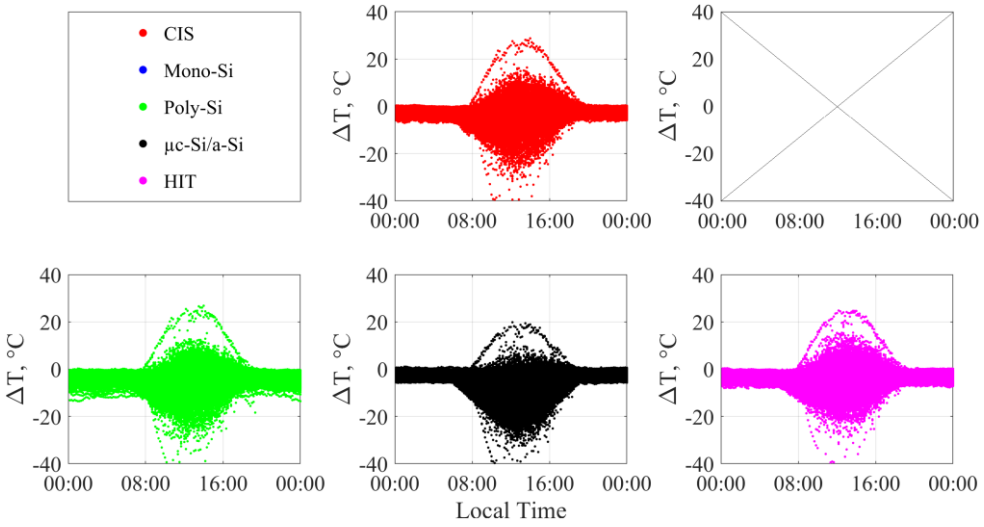

Fig. A4. Difference of module temperatures measured and estimated with Eq. (4).

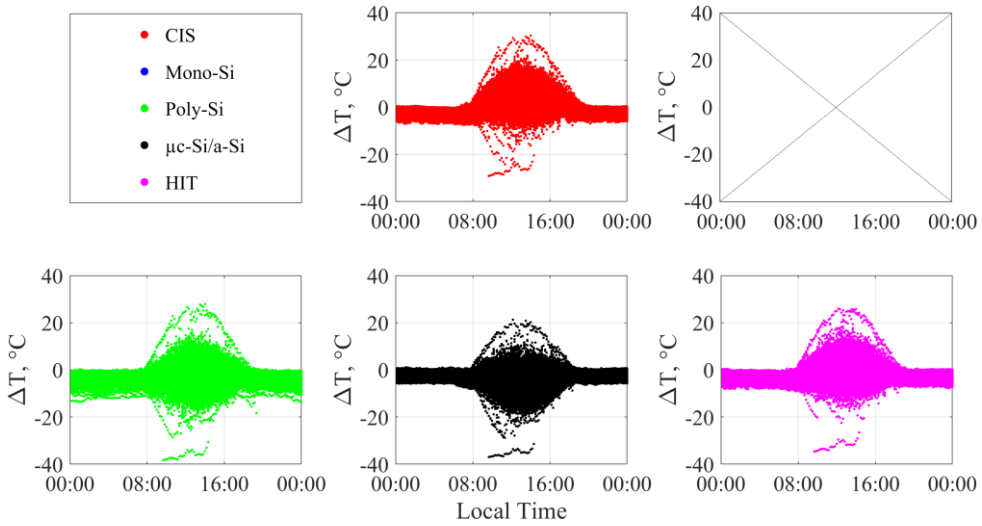

Fig. A5. Difference of module temperatures measured and estimated with Eq. (5).

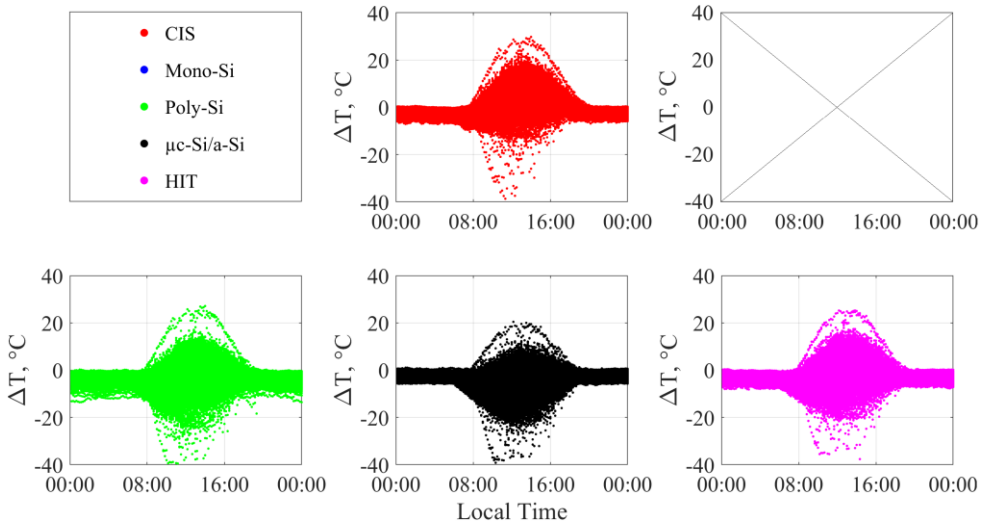

Fig. A6. Difference of module temperatures measured and estimated with Eq. (6).

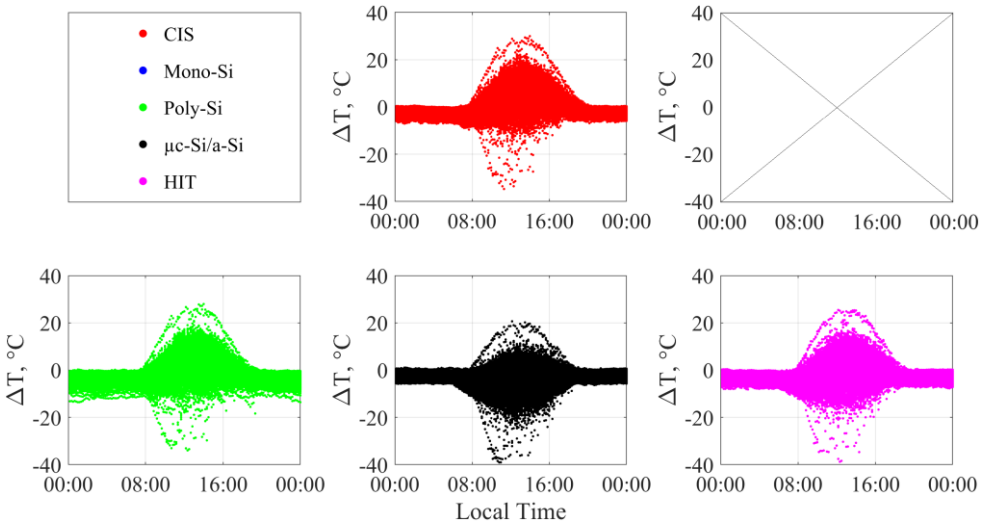

Fig. A7. Difference of module temperatures measured and estimated with Eq. (7).

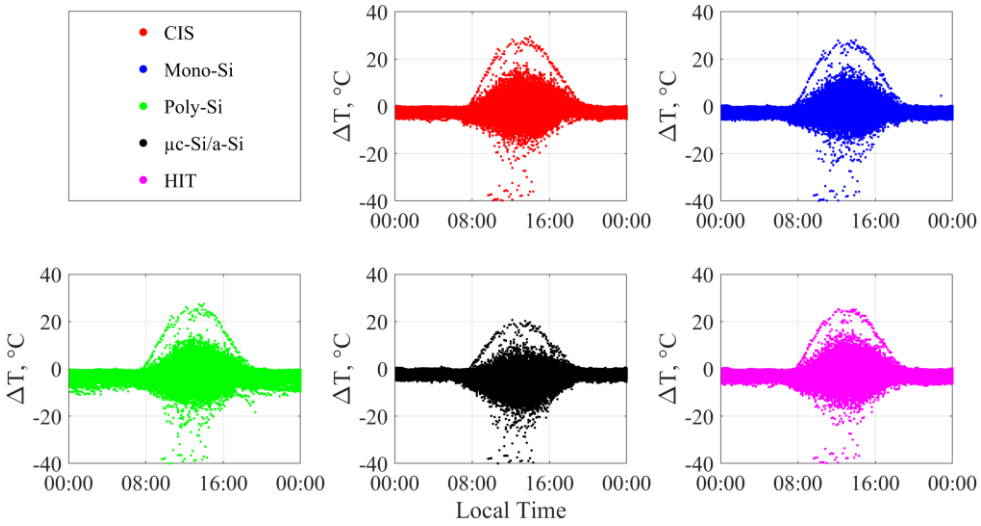

Fig. A8. Difference of module temperatures measured and estimated with Eq. (8).

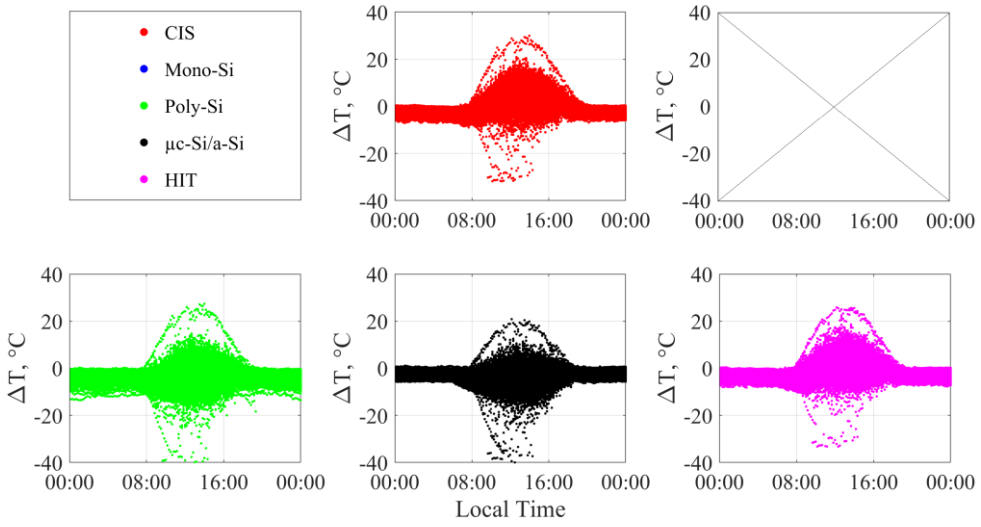

Fig. A9. Difference of module temperatures measured and estimated with Eq. (9).

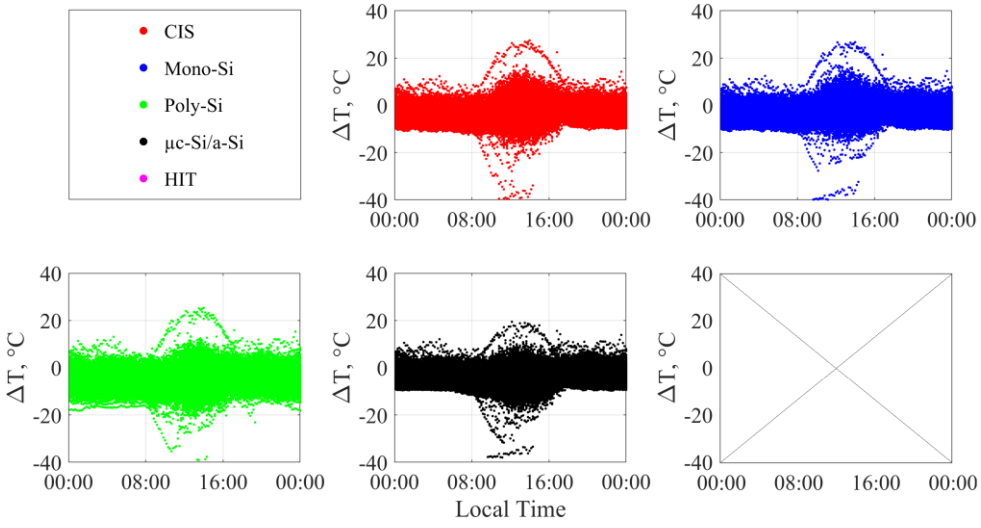

Fig. A10. Difference of module temperatures measured and estimated with Eq. (10).

REFERENCES

Akhsassi, M. *et al*. (2018). "Experimental Investigation and Modeling of the Thermal Behavior of a Solar PV Module." *Solar Energy Materials and Solar Cells*, Vol.180, pp. 271–79.

Amr, Ayman Abdel raheim, A. A.M. Hassan, Mazen Abdel-Salam, and Abou Hashema M. El-Sayed. (2019). "Enhancement of Photovoltaic System Performance via Passive Cooling: Theory versus Experiment." *Renewable Energy*, Vol.140, pp. 88–103.

Bañuelos-Ruedas, F., C. Angeles-Camacho, and S. Rios-Marcuello. (2010). "Analysis and Validation of the Methodology Used in the Extrapolation of Wind Speed Data at Different Heights." *Renewable and Sustainable Energy Reviews*, Vol.14, No.8, pp. 2383–2391.

Lo Brano, Valerio, and Giuseppina Ciulla. (2013). "An Efficient Analytical Approach for Obtaining a Five Parameters Model of Photovoltaic Modules Using Only Reference Data." *Applied Energy*, No.111, pp. 894–903.

Cole, R J, and N S Sturrock. (1977). "The Convective Heat Exchange at the External Surface of Buildings." *Building and Environment*, Vol.12, No.4, pp. 207–14.

Dierauf, Timothy, Aaron Growitz, Sarah Kurtz, and Clifford Hansen. (2013). "Weather-Corrected Performance Ratio Technical Report NREL/TP-5200-57991." *Technical Report, No. NREL/TP-5200-57991* NREL/TP-52, pp. 1–16.

Ding, Kun, Jingwei Zhang, Xingao Bian, and Junwei Xu. (2014). "A Simplified Model for Photovoltaic Modules Based on Improved Translation Equations." *Solar Energy*, Vol. 101, pp. 40–52.

Dubey, Swapnil, Jatin Narotam Sarvaiya, and Bharath Seshadri. (2013). "Temperature Dependent Photovoltaic (PV) Efficiency and Its Effect on PV Production in the World – A Review." *Energy Procedia*, Vol. 33, pp. 311–21.

Duffie, John A., and William A. Beckman. (2013). *Solar Engineering of Thermal Processes*, Wiley 4. Edition, New Jersey, USA.

Eckstein, Jürgen Helmut. (1990). "Detailed Modelling of Photovoltaic System Components." Master Thesis, University of Wisconsin-Madison.

Faiman, David. (2008). "Assessing the Outdoor Operating Temperature of Photovoltaic Modules." *Progress in Photovoltaics: Research And Applications*, Vol.16, pp. 307–15.

Gökmen, Nuri *et al*. (2016). "Investigation of Wind Speed Cooling Effect on PV Panels in Windy Locations." *Renewable Energy*, Vol. 90, pp. 283–90.

Homer Pro 3.13 Help Documentation, https://www.homerenergy.com/products/pro/docs/latest/how_homer_calculates_the_pv_cell_temperature.html [Accessed 20 Oct 2019].

IEA. (2019). Report: *PVPS 2019 Snapshot of Global PV Markets, Task 1: Strategic PV Analysis & Outreach*.

IRENA. (2019). Report: 1 International Renewable Energy Agency *Renewable Energy Statistics 2019*.

Kaplani, E, and S Kaplanis. (2014). "Thermal Modelling and Experimental Assessment of the Dependence of PV Module Temperature on Wind Velocity and Direction, Module Orientation and Inclination." *Solar Energy*, Vol. 107, pp. 443–60.

King, David L, William E Boyson, and Jay A Kratochvil. (2004). Report: *Photovoltaic Array Performance Model*, No: SAND2004-3, Springfield.

Koehl, Michael, Markus Heck, Stefan Wiesmeier, and Jochen Wirth. (2011). "Modeling of the Nominal Operating Cell Temperature Based on Outdoor Weathering." *Solar Energy Materials and Solar Cells*, Vol. 95, No. 7, pp. 1638–46.

Kurtz, Sarah *et al*. (2009). "Evaluation of High-Temperature Exposure of Rack-Mounted Photovoltaic Modules." *Conference Record of the IEEE Photovoltaic Specialists Conference*, Philadelphia, PA, USA, pp. 002399–002404.

Loveday, D L, and A H Taki. (1996). "Convective Heat Transfer Coefficients at a Plane Surface on a Full-Scale Building Facade." *International Journal of Heat and Mass Transfer*, Vol. 39, No. 8, pp.1729–42.

Mattei, M. *et al*. (2006). "Calculation of the Polycrystalline PV Module Temperature Using a Simple Method of Energy Balance." *Renewable Energy*, Vol. 31, No.4, pp. 553–67.

Nolay, Pierre. (1987). "Developpement d'une Methode Generale d'analyse Des Systemes Photovoltaiques.", PhD Thesis, ENMP, Paris, http://www.theses.fr/1987ENMP0052.

Ozden, Talat, Doga Tolgay, and Bulent G. Akinoglu. (2018). "Daily and Monthly Module Temperature Variation for 9 Different Modules." *PVCon 2018 - International Conference on Photovoltaic Science and Technologies*, Ankara, Turkey, Doi: 10.1109/PVCon.2018.8523878.

Peel, M. C., B. L. Finlayson, and T. A. McMahon. (2007). "Updated World Map of the Köppen-Geiger Climate Classification." *Hydrology and Earth System Sciences*, Vol. 11, No. 5, pp. 1633–44.

PVsyst 6 Help Doc. https://www.pvsyst.com/help/ [15 Oct 2019].

Rahman, M. M., M. Hasanuzzaman, and N. A. Rahim. (2015). "Effects of Various Parameters on PV-Module Power and Efficiency." *Energy Conversion and*

Management, Vol. 103, pp. 348–58.

Roberts, Justo José, Andrés A. Mendiburu Zevallos, and Agnelo Marotta Cassula. (2017). "Assessment of Photovoltaic Performance Models for System Simulation." *Renewable and Sustainable Energy Reviews*, Vol. 72, pp. 1104–23.

Ross, R.G., and M.I. Smokler. (1986). Repot: *Electricity from Photovoltaic Solar Cells: Flat-Plate Solar Array Project Final Report*. California.

Rubel, Franz, Katharina Brugger, Klaus Haslinger, and Ingeborg Auer. (2017). "The Climate of the European Alps: Shift of Very High Resolution Köppen-Geiger Climate Zones 1800-2100." *Meteorologische Zeitschrift*, Vol. 26, No: 2, pp. 115–25.

Sandnes, BjØrnar, and John Rekstad. (2002). "A Photovoltaic/Thermal (PV/T) Collector with a Polymer Absorber Plate. Experimental Study and Analytical Model." *Solar Energy*, Vol. 72, No. 1, pp. 63–73.

Santhakumari, Manju, and Netramani Sagar. (2019). "A Review of the Environmental Factors Degrading the Performance of Silicon Wafer-Based Photovoltaic Modules: Failure Detection Methods and Essential Mitigation Techniques." *Renewable and Sustainable Energy Reviews*, Vol. 110, pp. 83–100.

Schwingshackl, C. *et al*. (2013). "Wind Effect on PV Module Temperature: Analysis of Different Techniques for an Accurate Estimation." *Energy Procedia*, Vol. 40, pp. 77–86.

Sharples, S, and P S Charlesworth. (1998). "Full-Scale Measurements of Wind-Induced Convective Heat Transfer from a Roof-Mounted Flat Plate Solar Collector." *Solar Energy*, Vol. 62, No. 2, pp. 69–77.

Skoplaki, E., A. G. Boudouvis, and J. A. Palyvos. (2008). "A Simple Correlation for the Operating Temperature of Photovoltaic Modules of Arbitrary Mounting." *Solar Energy Materials and Solar Cells*, Vol. 92, No. 11, pp. 1393–1402.

Skoplaki, E., and J. A. Palyvos. (2009). "Operating Temperature of Photovoltaic Modules: A Survey of Pertinent Correlations." *Renewable Energy*, Vol. 34, No. 1, pp. 23–29.

SolarPowerEurope. (2018). Report: *Global Market Outlook*. EPIA - European Photovoltaic Industry Association.

Tamizhmani, Govindasamy *et al*. (2003). "Photovoltaic Module Thermal / Wind Performance : Long -Term Monitoring and Model Development For Energy Rating." *NCPV and Solar Program Review Meeting*, Denver, Colorado, pp. 936–39.

Twidell, John, and Tony Weir. (2015). *Renewable Energy Resources*. Taylor & Francis 3rd Editio. London.